

Lyapunov exponents in resonance multiplets

I. I. Shevchenko

Pulkovo Observatory of the Russian Academy of Sciences
Pulkovskoje ave. 65, St.Petersburg 196140, Russia

Abstract

The problem of estimating the maximum Lyapunov exponents of the motion in a multiplet of interacting nonlinear resonances is considered for the case when the resonances have comparable strength. The corresponding theoretical approaches are considered for the multiplets of two, three, and infinitely many resonances (i.e., doublets, triplets, and “infinities”). The analysis is based on the theory of separatrix and standard maps. A “multiplet separatrix map” is introduced, valid for description of the motion in the resonance multiplet under certain conditions. In numerical experiments it is shown that, at any given value of the adiabaticity parameter (which controls the degree of interaction/overlap of resonances in the multiplet), the value of the maximum Lyapunov exponent in the multiplet of equally-spaced equally-sized resonances is minimal in the doublet case and maximal in the infinity case. This is consistent with the developed theory.

Keywords: Hamiltonian dynamics; Chaotic dynamics; Resonances; Lyapunov exponents; Separatrix map; Standard map

1 Introduction

Calculating or estimating the Lyapunov exponents provides a powerful tool for exploring most fundamental properties of dynamical systems in various physical and mechanical applications. The main advantage of this tool is that

it allows one to separate chaos from order. If close trajectories in the bounded phase space diverge exponentially, then the motion is chaotic [1, 2, 3]. The maximum rate of this exponential divergence is characterized by the maximum Lyapunov exponent L . The quantity $T_L \equiv L^{-1}$ is the so-called Lyapunov time, representing the characteristic time of predictable dynamics. Knowledge of the Lyapunov time allows one to judge on the possibility for predicting the motion in chaotic domains of phase space. Due to the exponential divergence of chaotic orbits, the trajectory of any dynamical system cannot be accurately predicted on timescales much greater than system's Lyapunov time; this determines the importance of methods for estimating the Lyapunov exponents and times in physical and mechanical applications [1, 2, 4].

In this article, we consider the problem of estimating the maximum Lyapunov exponent of the motion in a multiplet of interacting resonances for the case when the resonances have comparable strength. For describing nonlinear resonances, we use the perturbed pendulum model (it was introduced in [1] as a “universal” one). Considering the case of interacting resonances of comparable strength is inspired by the fact that when one applies the perturbed pendulum model of nonlinear resonance in various applications, one usually finds out that the perturbations are not at all weak; see examples in [5].

2 Resonance multiplets

For the model of perturbed nonlinear resonance, we take the following paradigmatic Hamiltonian [6, 7]:

$$H = \frac{\mathcal{G}p^2}{2} - \mathcal{F} \cos \phi + a \cos(\phi - \tau) + b \cos(\phi + \tau). \quad (1)$$

The first two terms in Eq. (1) represent the Hamiltonian H_0 of the unperturbed pendulum, where ϕ is the pendulum angle (the resonance phase angle), and p is the momentum. The periodic perturbations are given by the last two terms; τ is the phase angle of perturbation: $\tau = \Omega t + \tau_0$, where Ω is the perturbation frequency, and τ_0 is the initial phase of the perturbation. The quantities \mathcal{F} , \mathcal{G} , a , b are constants. The frequency of the pendulum small-amplitude oscillations is given by

$$\omega_0 = (\mathcal{F}\mathcal{G})^{1/2}. \quad (2)$$

An important “adiabaticity parameter” [1], measuring the relative frequency of perturbation, is

$$\lambda = \frac{\Omega}{\omega_0}. \quad (3)$$

In the well-known phase portrait “ ϕ - p ” of the non-perturbed pendulum, a single domain (“cell”) of librations, bounded by the non-perturbed separatrix, is present. If the perturbations are “switched on” (i.e., $\varepsilon \neq 0$), a section of the phase space of motion can be constructed. Let us construct it at $\tau = 0 \bmod 2\pi$, taking the parameters’ values as follows: $\Omega = 8$, $\omega_0 = 1$, $a = b$, $\varepsilon \equiv \frac{a}{\mathcal{F}} = 0.5$. The resulting section is shown in Fig. 1; now not one but three domains of librations, i.e., three resonances, are present.

If the perturbation frequency is relatively large (as in Fig. 1, where $\lambda = 8$), the separation of resonances in the momentum p is large and they almost do not interact. On reducing the frequency of perturbation, the resonances approach each other and appreciable chaotic layers emerge in the vicinity of the separatrices (see Fig. 2, where $\lambda = 5$; the value of ε is as in the previous section). As it is well visible in Fig. 2, the motion in the vicinity of the separatrices is irregular. On reducing further the frequency of perturbation, the layers merge into a single chaotic layer, due to strong overlap of the resonances (see Fig. 3, where $\lambda = 2$).

3 The separatrix map

The chaotic layer theory has applications in various areas of physics, mechanics and, in particular, in celestial mechanics [1, 5]. The key role in this theory is played by the separatrix maps. They represent the motion of a system close to separatrices in a discrete way (“stroboscopically”): system’s state, set by the “time” and “energy” variables, is mapped discretely at the moments of passage of the positions of equilibrium by the pendulum describing the resonance.

The motion near the separatrices of the perturbed pendulum (1) with asymmetric perturbation ($a \neq b$) is described by the so-called separatrix algorithmic map [6]:

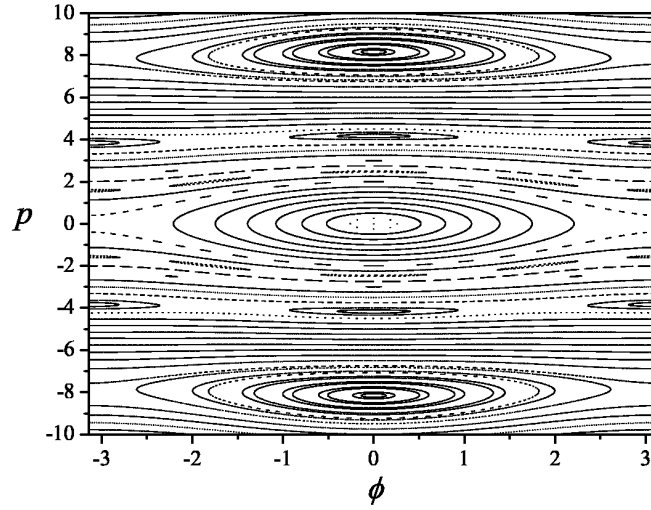


Figure 1: A chaotic resonance triplet. Weak interaction ($\lambda = 8$).

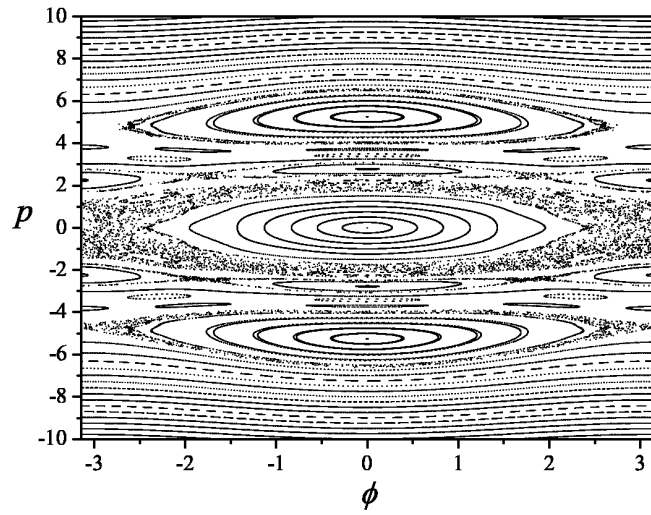


Figure 2: A chaotic resonance triplet. Moderate interaction ($\lambda = 5$).

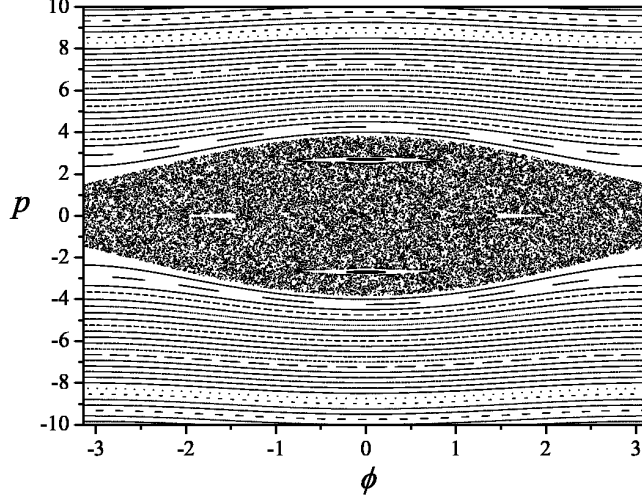


Figure 3: A chaotic resonance triplet. Strong overlap ($\lambda = 2$).

$$\begin{aligned}
&\text{if } w_i < 0 \text{ and } W = W^- \text{ then } W := W^+, \\
&\text{if } w_i < 0 \text{ and } W = W^+ \text{ then } W := W^-; \\
&w_{i+1} = w_i - W \sin \tau_i, \\
&\tau_{i+1} = \tau_i + \lambda \ln \frac{32}{|w_{i+1}|} \pmod{2\pi};
\end{aligned} \tag{4}$$

where λ is given by Eq. (3), and

$$\begin{aligned}
W^+(\lambda, \eta) &= \varepsilon \lambda (A_2(\lambda) + \eta A_2(-\lambda)), \\
W^-(\lambda, \eta) &= \varepsilon \lambda (\eta A_2(\lambda) + A_2(-\lambda)),
\end{aligned} \tag{5}$$

$\varepsilon = \frac{a}{\mathcal{F}}$, $\eta = \frac{b}{a}$. The Melnikov–Arnold integral (“MA-integral”) $A_2(\lambda)$ is given by the formula

$$A_2(\lambda) = 4\pi\lambda \frac{\exp(\pi\lambda/2)}{\sinh(\pi\lambda)}, \tag{6}$$

see [1, 8, 7].

The quantity w denotes the relative (with respect to the separatrix value) pendulum energy: $w \equiv \frac{H_0}{\mathcal{F}} - 1$. The variable τ is the phase angle of perturbation. One iteration of map (4) corresponds to one half-period of pendulum's libration or one period of its rotation.

If $a = b$ (the symmetric case), the separatrix algorithmic map reduces to the well-known ordinary separatrix map

$$\begin{aligned} w_{i+1} &= w_i - W \sin \tau_i, \\ \tau_{i+1} &= \tau_i + \lambda \ln \frac{32}{|w_{i+1}|} \pmod{2\pi}, \end{aligned} \quad (7)$$

first written in this form in [9, 1]; the expression for W [8, 7] is

$$W = \varepsilon \lambda (A_2(\lambda) + A_2(-\lambda)) = 4\pi\varepsilon \frac{\lambda^2}{\sinh \frac{\pi\lambda}{2}}. \quad (8)$$

Formula (8) differs from that given in [1, 2] by the term $A_2(-\lambda)$, which is small for $\lambda \gg 1$. However, its contribution is significant when λ is small [8], i.e., in the case of adiabatic chaos.

An equivalent form of Eqs. (7), used, e.g., in [10, 11], is

$$\begin{aligned} y_{i+1} &= y_i + \sin x_i, \\ x_{i+1} &= x_i - \lambda \ln |y_{i+1}| + c \pmod{2\pi}, \end{aligned} \quad (9)$$

where $y = w/W$, $x = \tau + \pi$; and

$$c = \lambda \ln \frac{32}{|W|}. \quad (10)$$

In [7], the theory of separatrix maps was shown to be legitimate for using to describe the motion near separatrices of perturbed nonlinear resonances in the full range of λ , including its low values. The half-width y_b of the main chaotic layer of the separatrix map (9) in the case of the least perturbed border of the layer was computed as a function of λ in [12, fig. 1]. The observed dependence follows a piecewise linear law with a transition point at $\lambda \approx 1/2$. This transition takes place not only in what concerns the width of the layer, but also in other characteristics of the motion, in particular, in the maximum Lyapunov exponent. The clear-cut sharp transition at this point manifests a qualitative distinction between two types of dynamics, “adiabatic” (“slow”) and “non-adiabatic” (“fast”) chaos [12].

The parameter $\lambda = \Omega/\omega_0$ measures the distance between the perturbing and guiding resonances in the units of one quarter of the width of the guiding resonance. Therefore, λ can be regarded as a kind of the resonance overlap parameter [13]. It is important to note that the border $\lambda \approx 1/2$ between the cases of adiabatic chaos and non-adiabatic chaos does not separate the cases of resonance overlap and resonance non-overlap: the border between the latter cases lies much higher in λ ; e.g., in the phase space of the standard map the integer resonances start to overlap, on decreasing λ , at $K_G = 0.9716\dots$ [1, 3], i.e., already at $\lambda = 2\pi/\sqrt{K_G} \approx 6.37$.

4 A multiplet separatrix map

Let us consider a nonlinear resonance in the perturbed pendulum model with several harmonic perturbations (i.e., in comparison with Hamiltonian (1), the number of equally-spaced perturbing harmonics may be arbitrary):

$$H = \frac{\mathcal{G}p^2}{2} - \mathcal{F} \cos \phi + \sum_{k=1}^M a_k \cos(\phi - k\tau) + \sum_{k=1}^M b_k \cos(\phi + k\tau). \quad (11)$$

Thus the number of resonances in the multiplet is equal to $2M + 1$.

Let us build a separatrix map for Hamiltonian (11) with the symmetric perturbations ($a_k = b_k$). If the perturbations are asymmetric, the problem is more complicated, because the separatrix map becomes algorithmic, as in the triplet case [6].

Setting $a_k = b_k$ and calculating the increment of the energy variable (analogously to the triplet case, considered in [1]) gives the result $\sum_{k=1}^M W_k \sin(k\tau_i)$, whereas the increment of the time variable remains the same as in the triplet case. Thus the separatrix map (7) is generalized to a “multiplet separatrix map”, given by

$$\begin{aligned} w_{i+1} &= w_i - \sum_{k=1}^M W_k \sin(k\tau_i), \\ \tau_{i+1} &= \tau_i + \lambda \ln \frac{32}{|w_{i+1}|} \pmod{2\pi}, \end{aligned} \quad (12)$$

where

$$W_k = 4\pi\varepsilon_k \frac{\lambda_k^2}{\sinh \frac{\pi\lambda_k}{2}},$$

where $\lambda_k = k\lambda$ and $\varepsilon_k \equiv \frac{a_k}{\mathcal{F}} = \frac{b_k}{\mathcal{F}}$.

The domain of validity of map (12) (in describing the near-separatrix motion) is expected to be usually much smaller than that of map (7), because the natural condition of validity $|W| \lesssim 1$ generalizes here to the condition $\sum_{k=1}^M |W_k| \lesssim 1$. Thus, if there is a lot of perturbing harmonics, the maximum allowed amplitudes ε_k in the multiplet case must be usually much smaller than the maximum allowed amplitude ε in the triplet case, at any given value of λ .

Also note that in the case of non-adiabatic perturbation ($\lambda \gtrsim 1/2$) the multiplet map (12) can be usually replaced by the classical map (7) for the “central” triplet (with $W = W_1$), because at high values of λ the coefficients W_k at $k > 1$ are exponentially small with k , with respect to W_1 .

5 Analytical estimating the Lyapunov exponents

The maximum Lyapunov exponent is defined by the formula

$$L = \limsup_{\substack{t \rightarrow \infty \\ d(t_0) \rightarrow 0}} \frac{1}{t - t_0} \ln \frac{d(t)}{d(t_0)}, \quad (13)$$

where $d(t_0)$ is the distance (in the phase space of motion) between two nearby initial conditions for two trajectories at the initial instant of time t_0 , and $d(t)$ is the distance between the evolved initial conditions at time t (e.g., [2]).

The art of calculation of the Lyapunov exponents (and, in particular, the maximum Lyapunov exponent) on computers has more than a thirty-year history and during this time it has become an extensive part of applied mathematics; see reviews in [14, 2]. Modern numerical methods for computation of the Lyapunov exponents are effective and precise. Approaches for analytical estimating the Lyapunov exponents were started to be developed relatively recently, beginning with those providing precision by the order of magnitude [15, 16], and later on providing precision comparable to the numerical methods [17, 18, 20, 21, 5, 22], though in limited applications.

Morbidelli and Froeschlé [15] and Nesvorný and Morbidelli [16, p. 256] suggested to estimate the Lyapunov time by taking it equal, by the order of magnitude, to the libration/circulation period of the resonant angle, or, in practice, to the period of small-amplitude oscillations on resonance (i.e., $\sim 1/\omega_0$). This estimate has a rather limited domain of validity; in fact, as we shall see in Section 6, $L \sim \omega_0$ solely at $\lambda \simeq 1$, and the ratio $L/\omega_0 \rightarrow 0$ in both limits $\lambda \rightarrow 0$ and $\lambda \rightarrow \infty$; besides, L/ω_0 rather strongly depends on other parameters, such as the perturbation amplitude ε .

A different approach, based on derivation of a discrete map for a triplet, was proposed by Holman and Murray [17, 18]. This is also a one-parameter approach, but using an effective resonance overlap parameter K_{eff} instead of ω_0 or Ω . The strength of perturbation is ignored, only frequencies are taken into account. In some way K_{eff} is analogous to the stochasticity parameter K of the standard map (whose theory is given in [1]), though K_{eff} was introduced for a triplet. Holman and Murray derived heuristic formulas for estimating the maximum Lyapunov exponent in the case of moderate resonance overlap, when $K_{\text{eff}} \sim 1$, and in the case of strong overlap (the adiabatic case), when $K_{\text{eff}} \gg 1$. In the first case, the maximum Lyapunov exponent was estimated in [17] as $L \approx \omega_0$ (the frequency of small oscillations on the resonance), and in the second case as $L \approx \Omega$ (the frequency of external perturbation). Murray and Holman [18] refined somewhat the formula in the case of strong overlap ($K_{\text{eff}} \gg 1$) by introducing a logarithmic dependence on K_{eff} , namely $L \propto \ln(K_{\text{eff}}/2)$, the function essentially the same as for the standard map (see Subsection 5.5), though derived for a triplet. For the whole range of resonance overlap, $1 < K_{\text{eff}} < +\infty$, they proposed the following interpolating formula¹:

$$L = \frac{\Omega}{2\pi} \ln \left(1 + \frac{K_{\text{eff}}}{4} + \left(\frac{K_{\text{eff}}}{2} + \left(\frac{K_{\text{eff}}}{4} \right)^2 \right)^{1/2} \right). \quad (14)$$

Let $K_{\text{eff}} = 1$ (this value belongs to the case of moderate overlap), then, taking $\Omega = 2\pi$, one has $L = \ln 2 \approx 0.69$. For the standard map, the actual value of L at $K = 1$ and $\Omega = 2\pi$ is ≈ 0.13 (as we shall see in Subsection 5.5, Eq. (26)), and for the triplet it is smaller. Thus Eq. (14) can be used for estimates solely by the order of magnitude, because the perturbation strength, asymmetry

¹There is a misprint in the original paper [18]. We quote the corrected formula, as given in [19, Eq. (12.14)].

of perturbation, and number of resonances in multiplets are ignored in it. It cannot be used in the case of weak interaction of resonances, when they do not overlap.

In [20, 21], an approach for estimating the maximum Lyapunov exponent of the chaotic motion in the vicinity of separatrices of a perturbed nonlinear resonance was proposed in the framework of the separatrix map theory. We follow the approach [20, 21], representing the maximum Lyapunov exponent L of the motion in the main chaotic layer of system (1) as the ratio of the maximum Lyapunov exponent L_{sx} of its separatrix map and the average period T of rotation (or, equivalently, the average half-period of libration) of the resonance phase ϕ inside the layer. For convenience, we introduce the non-dimensional quantity $T_{\text{sx}} = \Omega T$. Then the general expression for L is

$$L = \Omega \frac{L_{\text{sx}}}{T_{\text{sx}}}. \quad (15)$$

The quantity $T_{\text{L}} \equiv L^{-1}$, by definition, is the Lyapunov time.

In [5], the following four generic kinds of interacting resonances were considered: fast-chaotic resonance triplet, fast-chaotic resonance doublet, slow-chaotic resonance triplet, and slow-chaotic resonance doublet. Here we present formulas for the Lyapunov time T_{L} [5, 22] for these four cases, and then proceed to considering a fifth generic kind, that of infinitely many interacting resonances.

5.1 Fast chaos. Resonance triplet

Assume that $a = b$ and $\lambda > 1/2$ in Eq. (1). Then one has a symmetric triplet of interacting resonances, and chaos is non-adiabatic. Following [20, 21], we take the λ dependence of the maximum Lyapunov exponent of the separatrix map (9) in the form

$$L_{\text{sx}}(\lambda) \approx C_h \frac{2\lambda}{1 + 2\lambda}, \quad (16)$$

where $C_h \approx 0.80$ is Chirikov's constant [24]. The average increment of τ (proportional to the average libration half-period, or rotation period) in the chaotic layer is [1, 20, 21]:

$$T_{\text{sx}}(\lambda, W) \approx \lambda \ln \frac{32e}{\lambda|W|}, \quad (17)$$

where e is the base of natural logarithms.

Then, the Lyapunov time for the fast-chaotic resonance triplet [5] is given by

$$T_L = \frac{T_{\text{pert}}}{2\pi} \frac{T_{\text{sx}}}{L_{\text{sx}}} \approx T_{\text{pert}} \frac{(1+2\lambda)}{4\pi C_h} \ln \frac{32e}{\lambda|W|}, \quad (18)$$

where $T_{\text{pert}} = 2\pi/\Omega$ is the period of perturbation.

5.2 Fast chaos. Resonance doublet

In the completely asymmetric case, when $a = 0$ or $b = 0$, the maximum Lyapunov exponent can be found by averaging the contributions of all separate components of the chaotic layer [5]. The averaged (over the whole layer) value of the maximum Lyapunov exponent is the sum of weighted contributions of the layer components corresponding to librations, direct rotations and reverse rotations of the model pendulum. The weights are directly proportional to the times that the trajectory spends in the components, and, due to the supposed approximate ergodicity, to the relative measures of the components in the phase space. Then, the formula for the Lyapunov time for the fast-chaotic resonance doublet [5, 13] is given by

$$T_L \approx \frac{T_{\text{pert}}}{2\pi} \cdot \frac{\mu_{\text{libr}} + 1}{\mu_{\text{libr}} \frac{L_{\text{sx}}(2\lambda)}{T_{\text{sx}}(2\lambda, W)} + \frac{L_{\text{sx}}(\lambda)}{T_{\text{sx}}(\lambda, W)}}, \quad (19)$$

where $\mu_{\text{libr}} \approx 4$, and W , L_{sx} , and T_{sx} are given by formulas (8), (16), and (17).

5.3 Slow chaos. Resonance triplet

If $\lambda < 1/2$, the diffusion across the chaotic layer is slow, and on a short time interval the trajectory of the separatrix map (9) follows close to some current “guiding” curve [5, 22], and this allows one to estimate characteristics of the chaotic layer in a straightforward manner; in particular, the Lyapunov time for this resonance type is given by

$$T_L \approx \frac{T_{\text{pert}}}{2\pi} \left(\ln \left| 4 \sin \frac{c}{2} \right| + \frac{c}{\lambda} \right), \quad (20)$$

where $c = \lambda \ln \frac{32}{|W|}$ (Eq. (10)). This formula has specific limits of applicability [22], namely, the parameter c (approximately equal to $\lambda \ln \frac{4}{\lambda|\varepsilon|}$ in the adiabatic case) should not be close to $0 \bmod 2\pi$.

At $\lambda \ll 1$ one has $W \approx 8\varepsilon\lambda$, hence the approximate formula for the Lyapunov time is

$$T_L \approx \frac{T_{\text{pert}}}{2\pi} \ln \left| \frac{16}{\varepsilon\lambda} \sin \left(\frac{\lambda}{2} \ln \frac{4}{|\varepsilon|\lambda} \right) \right|. \quad (21)$$

5.4 Slow chaos. Resonance doublet

In this case, the separatrix algorithmic map (4) degenerates to the ordinary separatrix map (7) with $W \approx 4\varepsilon\lambda$, i.e., mathematically this case is equivalent to the case of slow-chaotic resonance triplet, but with a different (halved) value of W [5, 22]. The Lyapunov time is then given by

$$T_L \approx \frac{T_{\text{pert}}}{2\pi} \ln \left| \frac{32}{\varepsilon\lambda} \sin \left(\frac{\lambda}{2} \ln \frac{8}{|\varepsilon|\lambda} \right) \right|, \quad (22)$$

provided that the parameter c is not close to $0 \pmod{2\pi}$.

5.5 Lyapunov exponents in supermultiplets. The standard map theory

Let us assume that the number of resonances in a resonance multiplet is greater than 3. In applications, this number can be very large [19]; then, the multiplet is called a “supermultiplet”. If chaos is non-adiabatic ($\lambda \gtrsim 1/2$), then one can apply, as an approximation, the formulas given in Subsections 5.1 and 5.2 for the triplet and doublet (depending on the perturbation asymmetry) cases, because the influence of the “far away” resonances is exponentially small with λ . However, if chaos is adiabatic ($\lambda \lesssim 1/2$), the triplet or doublet approximations do not work and one has to develop a different approach. Let us consider a limiting case, namely, the case of infinitely many interacting equally-sized equally-spaced resonances.

The standard map

$$\begin{aligned} y_{i+1} &= y_i + K \sin x_i \pmod{2\pi}, \\ x_{i+1} &= x_i + y_{i+1} \pmod{2\pi} \end{aligned} \quad (23)$$

describes the motion in an infinite multiplet of equally-sized equally-spaced resonances, as it is clear from its Hamiltonian [1]:

$$H = \frac{y^2}{2} + \frac{K}{(2\pi)^2} \sum_{k=-N}^N \cos(x - kt), \quad (24)$$

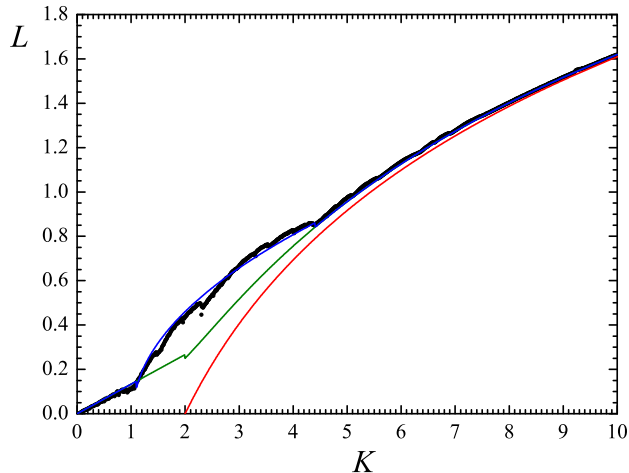


Figure 4: The dots show the numerical-experimental dependence $L(K)$ for the standard map at $0 < K < 10$, according to [23, 24]. The lower curve shows the function $\ln \frac{K}{2}$. The middle curve shows the glued functions (25), and the upper curve is given by Eq. (26), where $T_{\text{pert}} = 1$.

where $N = \infty$. The variables x_i, y_i of map (23) correspond to the variables $x(t_i), y(t_i)$ of the continuous system (24) taken stroboscopically at time moduli 2π (see, e.g., [1]).

The asymptotic formula for the maximum Lyapunov exponent of the standard map at $K \gg 1$ was derived in [1]: $L \propto \ln \frac{K}{2}$. Rather precise fitting formulas were obtained in [23, 24] for the $L(K)$ dependence at $K < 1$ and $K > 4.5$:

$$L = \frac{1}{T_{\text{pert}}} \cdot \begin{cases} 0.1333K, & \text{if } K < 1, \\ \ln \frac{K}{2} + \frac{1}{K^2}, & \text{if } K > 4.5, \end{cases} \quad (25)$$

where $K = (2\pi/\lambda)^2$. The functions (25) are depicted in Fig. 4. In this plot, they are glued at $K = 2$; this trick apparently results in underestimating the actual values of L in the interval $1 \lesssim K \lesssim 4.5$. Arranging a better fit for $L(K)$ at this interval, one arrives at the formulas

$$L = \frac{1}{T_{\text{pert}}} \cdot \begin{cases} 0.1333K, & \text{if } K < 1.1, \\ 0.469(K - 1.037)^{1/2}, & \text{if } 1.1 \leq K < 4.4, \\ \ln \frac{K}{2} + \frac{1}{K^2}, & \text{if } K \geq 4.4, \end{cases} \quad (26)$$

which describe the behavior of $L(K)$ at $1 \lesssim K \lesssim 4.5$ (corresponding to $3.0 \lesssim \lambda \lesssim 6.3$) much more accurately.

Thus the Lyapunov time in the “infinite” case is given by

$$T_L \approx T_{\text{pert}} \cdot \begin{cases} \frac{7.50}{K} (\approx 0.190\lambda^2), & \text{if } K < 1.1 \text{ (or, if } \lambda > 6.0), \\ 2.133(K - 1.037)^{-1/2}, & \text{if } 1.1 \leq K < 4.4 \text{ (or, if } 3.0 < \lambda \leq 6.0), \\ \left(\ln \frac{K}{2} + \frac{1}{K^2} \right)^{-1}, & \text{if } K \geq 4.4 \text{ (or, if } \lambda \leq 3.0), \end{cases} \quad (27)$$

where

$$K = (2\pi/\lambda)^2. \quad (28)$$

A well-known important constant of the standard map dynamics is the critical value of the parameter K , namely, $K_G = 0.971635406\dots$; see, e. g., [3]. It is obvious from Figs. 4 and 5, that at $K \lesssim 1$, i.e., at K below its approximate critical value, the dependence $L(K)$, if smoothed, is close to linear. This is explainable in the framework of the separatrix map theory [23]. Indeed, one can find the maximum Lyapunov exponent here using formula (18) for the fast-chaotic resonance triplet, because at $K \lesssim 1$ one has $\lambda \gtrsim 6$ and therefore the perturbing resonances non-neighboring the guiding one can be ignored in the first approximation (their contribution is considered below). Thus $L = \Omega L_{\text{sx}}/T_{\text{sx}}$ (Eq. (15)), where L_{sx} is given by Eq. (16) and T_{sx} is given by Eq. (17). As follows from Eq. (16), L_{sx} is practically constant at $\lambda \gtrsim 6$. On the other hand, T_{sx} is directly proportional to K^{-1} at small enough values of K , as follows from Eq. (17) (or see Eq. (6.18) in [1]). Therefore, $L \propto K$ at small enough values of K . However, this linear asymptotic behavior has a slope somewhat less than the average one adopted in approximation (26), where $L \approx 0.1333K$. Indeed, a careful inspection of Fig. 5 indicates that the slope of the smoothed dependence decreases with K .

Let us derive a formula for $L(K)$ at $0 \leq K \lesssim 1$. This will be a formula for the upper envelope of the observed “ragged” dependence (which

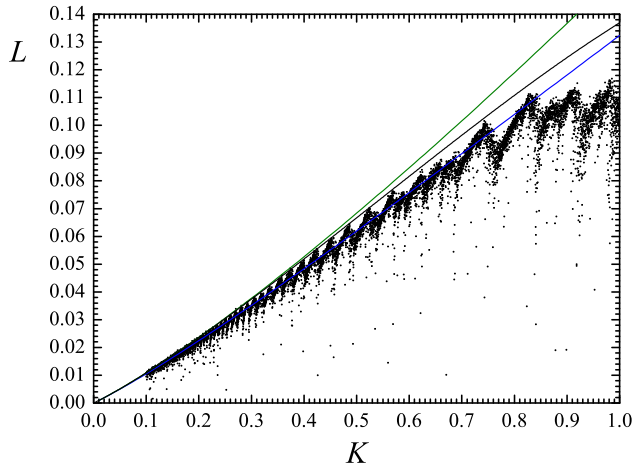


Figure 5: The numerical-experimental $L(K)$ dependence (dots) for the standard map [23, 24] at $0 < K < 1$. The lower solid curve is given by the separatrix map theory without any correction to the MA-integral; the upper solid curve is given by the separatrix map theory with the Chirikov zero-order correction to the MA-integral; the middle solid curve is given by the separatrix map theory with the Chirikov–Lazutkin–Gelfreich correction to the MA-integral.

has sharp local minima due to marginal resonances at the borders of the chaotic layer), because our theory (described in Section 5.1) is valid in the absence of marginal resonances. (The role of marginal resonance in defining the width of the chaotic layer is described in [8, 25, 26].)

We proceed from the basic relation (15) $L = \Omega \frac{L_{\text{sx}}}{T_{\text{sx}}}$, where $\Omega = 2\pi$, L_{sx} is given by Eq. (16), and T_{sx} is given by Eq. (17). However, we modify the expression for W , which enters in Eq. (17), changing W to $W_{\text{st}} = R_{\text{st}}W$, where R_{st} is a correction factor, introduced by Chirikov [1] to account for specific properties of the standard map. Thus the formula for T_{sx} attains the form

$$T_{\text{sx}} = \lambda \ln \frac{32e}{\lambda R_{\text{st}} |W|}. \quad (29)$$

Expressing λ through K , one arrives at a formula, derived in [1] for the average half-period of librations (or, the average period of rotations) in the chaotic layer of the integer resonance of the standard map; this formula is as follows:

$$T_{\text{sx}} = \Omega \left(\frac{\pi^2}{K} - K^{-1/2} \ln \frac{2R_{\text{st}}\pi^4}{eK^{3/2}} \right). \quad (30)$$

The introduction of the correction factor R_{st} is necessary for the separatrix-map correct description of the chaotic layer of the integer resonance of the standard map. Chirikov's numerical-experimental estimate of the correction factor gave $R_{\text{st}} \approx 2.15$ [1]. Later on, this factor was found out [27, 28] to be expressed through the so-called Lazutkin splitting constant: $R_{\text{st}} = f_0/(16\pi^3) \approx 2.2552$, where the Lazutkin constant $f_0 = 1118.8277059409008\dots$.

At non-zero K , the stable and unstable separatrices of the integer resonance of the standard map intersect transversally; Lazutkin [29] obtained an asymptotic (at $K \ll 1$) formula for the separatrix splitting angle. The splitting angle at the first intersection of the separatrices with the line $x = \pi$ is given by

$$\alpha = \frac{\pi}{h^2} \exp \left(-\frac{\pi^2}{h} \right) \sum_{m=0}^{\infty} c_m h^{2m}, \quad (31)$$

where

$$h = \ln \left(1 + \frac{K}{2} + \left(K + \frac{K^2}{4} \right)^{1/2} \right), \quad (32)$$

and the first three coefficients c_m are given by the formulas

$$c_0 = f_0, \quad c_1 = f_1 - \frac{c_0}{4}, \quad c_2 = f_2 - \frac{c_1}{4} - \frac{25c_0}{72}, \quad (33)$$

where

$$f_0 = 1118.8277059\dots, \quad f_1 = 18.59891\dots, \quad f_2 = -2.17205\dots \quad (34)$$

[29, 30]. Taking into account the asymptotic expansion (31), one arrives at

$$R_{\text{st}} \approx \frac{1}{16\pi^3} (c_0 + c_1 h^2 + c_2 h^4), \quad (35)$$

where $h \approx K^{1/2}$.

Combining Eqs. (15), (16), (29), and (35), we build a theoretical $L(K)$ curve; it is the middle solid one in Fig. 5. For comparison, the lower solid curve in this Figure is given by the separatrix map theory without any correction to the MA-integral (i.e., $R_{\text{st}} = 1$), and the upper solid curve is given by the separatrix map theory with the Chirikov zero-order (in h) correction to the MA-integral (i.e., $R_{\text{st}} = 2.2552$). One can see that the middle curve, built on the basis of the most refined theory, provides the best approximation for the upper envelope of the numerical-experimental relationship, as expected.

6 Theory versus numerical experiment

In this Section we verify our theoretical results versus numerical simulations. For computing the maximum Lyapunov exponent (and, generally, the Lyapunov spectra) we use the algorithms and software developed in [31, 32] on the basis of the HQRB numerical method by von Bremen et al. [34] for calculation of the Lyapunov spectra. The HQRB method is based on the QR decomposition of the tangent map matrix using the Householder transformation. For computing the trajectories we use the integrator by Hairer et al. [33], realizing an explicit 8th order Runge–Kutta method (with the step size control) due to Dormand and Prince.

Let us consider first of all a small perturbation amplitude, namely, we set $\varepsilon_k = \varepsilon = 0.01$ in Eq. (11). The corresponding λ dependences of the maximum Lyapunov exponent, normalized by ω_0 , are shown in Fig. 6 for the triplet case ($M = 1$ in Eq. (11)) and for the septet case ($M = 3$ in Eq. (11)). The dots and triangles denote the numerical-experimental data obtained for the triplet and septet, respectively. The thin curves show the numerical-experimental data obtained by iterations of the multiplet separatrix map (12), solid and dashed for the triplet and septet, respectively. The thick solid curve represents the separatrix map theory (given by Eqs. (18) and (21)) for the triplet. One can see that the theory is impressively good for the triplet. No theory is yet available for the septet; however, the multiplet separatrix map data and the results of direct numerical integrations are in obviously good agreement. At $\lambda \gtrsim 0.5$, i.e., in the domain of non-adiabatic chaos, the theory for the fast-chaotic triplet works good for both triplet and septet, because the perturbing role of the harmonics farther than the neighbors of the guiding resonance is

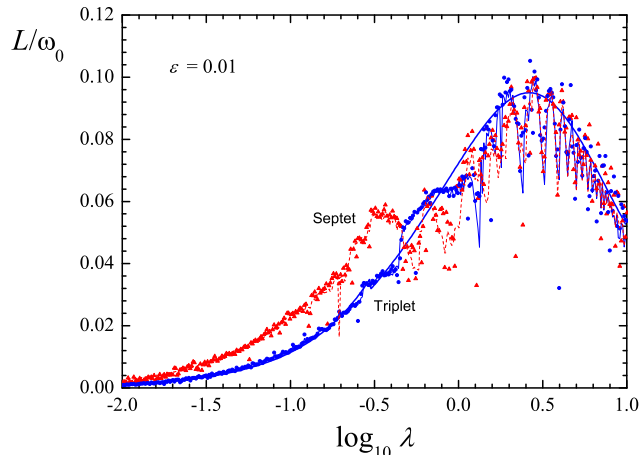


Figure 6: The λ dependences of the maximum Lyapunov exponent, normalized by ω_0 , in the triplet and septet cases; $\varepsilon_k = \varepsilon = 0.01$. The dots and triangles show the numerical-experimental data obtained for the triplet and septet, respectively, by means of numerical integrations of the equations of motion. The thin solid and dashed curves show the numerical-experimental data obtained by iterations of the multiplet separatrix map for the triplet and septet, respectively. The thick solid curve represents the separatrix map theory (given by Eqs. (18) and (21)) for the triplet.

negligible.

Now let us consider the ultimately large perturbation amplitude, namely, $\varepsilon_k = \varepsilon = 1$; in other words, let us consider equally-sized equally-spaced multiplets. We call the amplitude $\varepsilon = 1$ ultimately large, because the case of $\varepsilon > 1$ can be reduced to the case of $\varepsilon < 1$ by changing the choice of the guiding resonance.

The standard map theory, given by formulas (26) and (27), can be presumably applied for estimating the maximum Lyapunov exponents in multiplets of equally-sized equally-spaced resonances, when the number of resonances is large, assuming that the limiting case $M = \infty$ describes the situation at $M \gg 1$.

The λ dependences, both theoretical and numerical-experimental, of the maximum Lyapunov exponent (normalized by ω_0) for several multiplets of

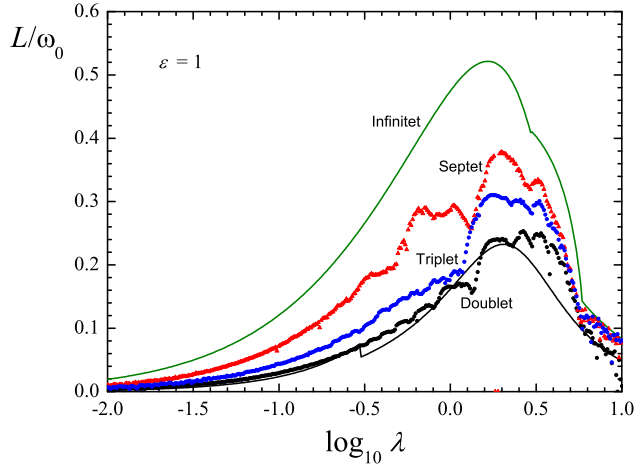


Figure 7: The λ dependences of the maximum Lyapunov exponent, normalized by ω_0 , for multiplets of equally-sized equally-spaced resonances. The dots show numerical-experimental data, and the curves show theoretical functions. The upper solid curve, given by Eqs. (26) and (28), represents the standard map theory for the infinitet; and the lower solid curve, given by Eqs. (19) and (22), represents the separatrix map theory for the doublet.

equally-sized equally-spaced resonances are shown in Fig. 7. One can see that the dependence for the septet occupies an intermediate (in the vertical axis) position between the dependence for the doublet and the dependence for the “infinitet”, i.e., for the standard map. The numerical data for the doublet agrees well with the separatrix map theory presented in Subsections 5.2 and 5.4, notwithstanding the large perturbation amplitude $\varepsilon = 1$.

Comparing the heights of the curves maxima in Fig. 6 (where $\varepsilon = 0.01$) and Fig. 7 (where $\varepsilon = 1$), one can see that L/ω_0 depends strongly on the perturbation amplitude ε , the difference being obvious (about three times). This emphasizes the fact that taking into account solely the frequencies Ω and ω_0 is insufficient for analytical estimates of L : the perturbation strength must be also taken into account whenever more or less precise estimates of L are sought for.

Inspecting the plots in Fig. 7 allows one to qualitatively estimate the

relative range of the Lyapunov exponent values between the doublet, triplet and infinitet cases. Let us designate the Lyapunov exponents for these three cases as $L^{(2)}$, $L^{(3)}$, and $L^{(\infty)}$, respectively. One can see that at $\lambda \sim 1-3$, i.e., where the values of L/ω_0 are maximal, the ratios $L^{(\infty)}/L^{(2)}$ and $L^{(\infty)}/L^{(3)}$ are of the order of 2. At the maxima of the curves, they are equal to 2.2 and 1.7, respectively.

It is also of interest how do the ratios $L^{(\infty)}/L^{(2)}$ and $L^{(\infty)}/L^{(3)}$ behave in the limits $\lambda \rightarrow 0$ and $\lambda \rightarrow \infty$, though L/ω_0 tends to zero in the both limits. Consider first the limit $\lambda \rightarrow \infty$. From Eqs. (19) and (18) the following asymptotic relations are easily derived for the fast-chaotic doublet and triplet cases, respectively:

$$\frac{T_L^{(2)}}{T_{\text{pert}}} = \frac{\mu_{\text{libr}} + 1}{2C_h(\mu_{\text{libr}} + 2)}\lambda^2 \approx \frac{5}{12C_h}\lambda^2 \approx 0.521\lambda^2 \quad (36)$$

and

$$\frac{T_L^{(3)}}{T_{\text{pert}}} = \frac{1}{4C_h}\lambda^2 \approx 0.313\lambda^2. \quad (37)$$

Thus

$$\frac{L^{(3)}}{L^{(2)}} = 2\frac{\mu_{\text{libr}} + 1}{\mu_{\text{libr}} + 2} \approx 5/3 \approx 1.67 \quad (38)$$

asymptotically. As pointed out in Subsection 5.5, it is expected that $L^{(\infty)} = L^{(3)}$ at $\lambda \rightarrow \infty$; therefore, $L^{(\infty)}/L^{(2)} \approx 1.67$ as well.

Note that the asymptotic behavior of $T_L^{(3)}/T_{\text{pert}}$, given by Eq. (37), is somewhat different from the average behavior of $T_L^{(\infty)}/T_{\text{pert}}$ (on the interval $0 < K(= (2\pi/\lambda)^2) < 1.1$), expressed in Eq. (27). Indeed, according to Eq. (27), at $\lambda \gtrsim 6$ one has $T_L^{(\infty)}/T_{\text{pert}} \approx 0.190\lambda^2$; i.e., the coefficient at λ^2 is 1.65 times less. The difference is explained by the fact that the linear-looking smoothed $L(K)$ dependence for the standard map at $0 < K < 1$ actually has the slope that weakly decreases with K , as also pointed out in Subsection 5.5.

Thus, as followed from Eq. (38), at $\lambda \rightarrow \infty$ one expects $L^{(\infty)}/L^{(2)} \approx 1.67$; in other words, the relative range of the Lyapunov exponent values, if λ is large, is rather narrow: the Lyapunov exponent in the infinitet is only about 70% greater than that in the doublet.

The range does not seem to be so narrow at all in the opposite (adiabatic) limit $\lambda \rightarrow 0$. Indeed, from Eqs. (22), (21) and (27) one finds in this limit

that $L^{(\infty)}/L^{(2)} \rightarrow \infty$ (whereas $L^{(3)}/L^{(2)} \rightarrow 1$). However note that this fact is not of much importance for applications, because $L/\omega_0 \rightarrow 0$ at $\lambda \rightarrow 0$.

Concluding this Section, let us discuss the effect of the perturbation strength in more detail. For the perturbation amplitudes $\varepsilon \sim \lambda^{-1}$ and above the standard Poincaré–Melnikov method for calculating the effects associated with the separatrix splitting generally requires corrections [35, 36]. What if the perturbation is ultimately large, i.e., $\varepsilon = 1$? In the doublet case, the perturbation is completely asymmetric ($\eta = 0$) and for this reason, according to [35], the correction is zero. For the triplet of arbitrary asymmetry, the correction factor R to the separatrix map parameter W for system (1), according to the Simó hypothetical formula [35], is $|R(x)| = \left| \frac{\sinh(x)}{x} \right|$, where $x \equiv (2\varepsilon_1\varepsilon_2)^{1/2} = \frac{(2ab)^{1/2}}{\mathcal{F}}$. (The value of x may be either real or imaginary, depending on the signs of a and b . The value of W is corrected by means of multiplying it by R ; i.e., the product RW is used instead of W .) In the symmetric triplet case, $\eta = 1$ and the correction factor is $R(\sqrt{2}) \approx 1.3683$. Thus the correction factor in the case of three equally-sized equally-spaced resonances is significantly smaller than that in the case of infinitely many equally-sized equally-spaced resonances, where $R \approx 2.2552$ (see Subsection 5.5).

Fig. 8 shows the λ dependences of the maximum Lyapunov exponent, normalized by ω_0 , for the cases of equally-sized doublet and equally-sized equally-spaced triplet. The dots show numerical-experimental data, and the solid curves show theoretical functions. The lower solid curve represents the separatrix map theory (given by Eqs. (19) and (22)) for the doublet. The upper solid curve represents the separatrix map theory for the triplet (given by Eqs. (18) and (21)) with the Simó correction; the middle thin dashed curve is the same but without the Simó correction. One can see that taking into account the Simó correction provides a much better fit to the numerical data, as expected.

Note that the resonances in the infinitet (the case of the standard map) start to overlap, on decreasing λ , at $K_G \approx 0.9716$ [1, 3], i.e., at $\lambda = 2\pi/\sqrt{K_G} \approx 6.37$ (see Section 3). Therefore, the ranges in λ in Figs. 6–8 almost completely correspond to the overlap condition, except at $\lambda \gtrsim 6.4$, i.e., at $\log_{10} \lambda \gtrsim 0.8$.

The basic conclusion following from our numerical experiments, described in this Section, is that at any given value of the adiabaticity parameter λ (which controls the degree of interaction/overlap of resonances in the resonance multiplet) the value of the maximum Lyapunov exponent in the mul-

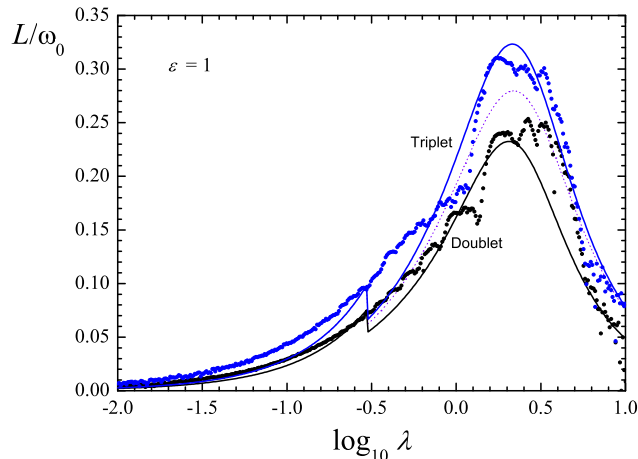


Figure 8: The λ dependences of the maximum Lyapunov exponent, normalized by ω_0 , for the cases of equally-sized doublet and equally-sized equally-spaced triplet. The dots show numerical-experimental data, and the curves show theoretical functions. The lower solid curve represents the separatrix map theory (given by Eqs. (19) and (22)) for the doublet. The upper solid curve represents the separatrix map theory for the triplet (given by Eqs. (18) and (21)) with the Simó correction; the middle thin dashed curve is the same but without the Simó correction.

triplet of equally-spaced equally-sized resonances is minimal in the doublet case and maximal in the infinitet case. This is consistent with the separatrix map and standard map theories: as it is clear from Fig. 7, the theoretical curves for the doublet and infinitet serve as the lower and upper bounds for all our numerical data on the Lyapunov exponents in the multiplets.

7 An example of application

Resonances with planets are ubiquitous in the motion of asteroids (see, e.g., [19]); of particular interest are the so-called mean motion resonances with Jupiter, i.e., the resonances between orbital periods of an asteroid and Jupiter (note that Jupiter is the largest planet in the Solar system and is closest,

among the giant planets, to the main asteroid belt; “mean motion” is the mean orbital frequency). The Hamiltonian of the motion of an asteroid with negligible mass in the gravitational field of the Sun and Jupiter, in the plane of Jupiter’s orbit, in the vicinity of a high-order mean motion resonance with Jupiter, can be approximated [17, 18] in the perturbed pendulum model as

$$H = \frac{1}{2}\beta\Lambda^2 - \sum_{p=0}^q \phi_{k+q, k+p, k} \cos(\psi - p\omega_1), \quad (39)$$

where $\Lambda = \Psi - \Psi_{\text{res}}$, $\Psi = (\mu_1 a)^{1/2}/k$, $\Psi_{\text{res}} = (\mu_1^2/(k^2(k+q)n_J))^{1/3}$. The leading resonant angle $\psi \equiv kl - (k+q)l_J$, where l and l_J are the mean longitudes of an asteroid and Jupiter. (Definitions of the orbital elements see, e.g., in [19].) The action-like variable Λ is canonically conjugated to ψ . The quantity $\beta = 3k^2/a^2$ is assumed to be a constant parameter; a and e are asteroid’s semimajor axis and eccentricity; $\omega_1 \equiv -\varpi$, i.e., ω_1 is minus the longitude of asteroid’s perihelion; its time derivative is assumed to be constant. The units are chosen in such a way that the gravitational constant, the total mass (Sun plus Jupiter), and Jupiter’s semimajor axis a_J are all equal to 1; Jupiter’s mass in the total mass units is $\mu = 1/1047.355$; $\mu_1 = 1 - \mu$. Jupiter’s mean motion $n_J = 1$; i.e., the adopted time unit is equal to $\frac{1}{2\pi}$ th part of Jupiter’s orbital period.

The integer non-negative numbers k and q define the resonance: the ratio $(k+q)/k$ is equal to the ratio of mean motions of an asteroid and Jupiter in the exact resonance; q is the resonance order. According to Eq. (39), the mean motion resonance $(k+q)/k$ splits in a cluster of $q+1$ subresonances $p = 0, 1, \dots, q$. For the coefficients of the resonant terms one has

$$|\phi_{k+q, k+p, k}| \approx \frac{\mu}{q\pi a_J} \binom{q}{p} \left(\frac{\epsilon}{2}\right)^p \left(\frac{\epsilon_J}{2}\right)^{q-p}, \quad (40)$$

where $\epsilon \equiv ea_J/(a_J - a)$, $\epsilon_J \equiv e_J a_J/(a_J - a)$. Jupiter’s current eccentricity is $e_J = 0.048$. The frequency of small-amplitude oscillations on subresonance p is

$$\omega_0 = (\beta|\phi_{k+q, k+p, k}|)^{1/2} \approx \frac{a_J}{a_J - a} n_J \left(\mu_1 \mu \frac{4q}{3\pi} \binom{q}{p} \left(\frac{a}{a_J}\right) \left(\frac{\epsilon}{2}\right)^p \left(\frac{\epsilon_J}{2}\right)^{q-p} \right)^{1/2}, \quad (41)$$

and the perturbation frequency is

$$\Omega = \dot{\omega}_1 \approx \frac{\mu_1 \mu}{2\pi} n_J \left(\frac{a}{a_J} \right)^{1/2} \left(\frac{a_J}{a_J - a} \right)^2, \quad (42)$$

cf. [17, 18].

As an example we take asteroid 522 Helga, which is famous to exhibit “stable chaos” [37, 38, 39, 5]: i.e., its computed Lyapunov time is rather small (~ 7000 yr), but numerical experiments do not reveal any gross changes of its orbit on cosmogonic time scales. Helga is known to be in the 12/7 mean motion resonance with Jupiter. We take necessary data on a , e , and the perihelion frequency $g = \dot{\varpi}$ for this asteroid in the “numb.syn” catalogue [40, 41] of the AstDyS web service². The value of T_{pert} is defined by the value of g ; thus one finds $T_{\text{pert}} = 6700$ yr.

To apply the separatrix map theory, one should identify the guiding sub-resonance in the multiplet. As such, it is natural to choose the subresonance that has the maximum amplitude (i.e., the maximum value of $|\phi_{k+q, k+p, k}|$). We find that the guiding subresonance in the sextet is the third one ($p = 2$), consequently the perturbing neighbors have numbers $p = 1$ and 3. Thus we find the separatrix map parameters: $\lambda = \Omega/\omega_0 = 2.32$, $\eta = 0.81$. Therefore, we model the multiplet by a fast-chaotic triplet. The relative strength of perturbation is rather strong: $\varepsilon = 0.79$. Applying Eq. (18), one has $T_L \approx 9800$ yr.

On the other hand, the standard map theory gives an estimate for the Lyapunov time from below. According to Eq. (28), $K = (2\pi/\lambda)^2$; thus one has for 522 Helga: $K \approx 7.3$, and, as follows from Eq. (27), $T_L \approx 5100$ yr.

Values of the Lyapunov time, computed in integrations in the full (accounting for perturbations from all major planets) problem are 6900 yr [38] and 6860 yr (AstDyS). Obviously, the standard map theory is closer to these “actual” values. This is because the number of resonances in the multiplet is large and the relative strength of perturbation ε is not far from 1, i.e., to the value characteristic for the standard map Hamiltonian.

8 Conclusions

In this article, the problem of estimating the maximum Lyapunov exponents of the motion in a multiplet of interacting resonances has been considered for

²<http://hamilton.dm.unipi.it/astdys/>

the case when the resonances have comparable strength. The corresponding theoretical approaches have been considered for the multiplets of two, three, and infinitely many interacting resonances (i.e., doublets, triplets, and “infinities”). The analysis has been based on the theory of separatrix and standard maps. We have introduced a “multiplet separatrix map”, valid for description of the motion in the resonance multiplet under certain conditions.

The separatrix map approach is suitable for the multiplet of any number of resonances, when their interaction is weak or moderate (i.e., the separation of resonances with respect to their sizes is large enough), as well as for the multiplet of two or three resonances (doublet or triplet), when the degree of interaction is arbitrary, including the case of strong overlap. The standard map approach is suitable for the multiplet of a large number of equally-sized equally-spaced resonances with arbitrary degree of interaction/overlap.

We have presented explicit analytical formulas for the Lyapunov times for the following five generic resonance multiplet types: fast-chaotic resonance triplet, fast-chaotic resonance doublet, slow-chaotic resonance triplet, slow-chaotic resonance doublet, and, for both cases of fast and slow chaos, infinity of equally-sized equally-spaced resonances. Good performance of the presented analytical formulas in the domains of their validity has been demonstrated by means of comparison with direct numerical integrations of the original Hamiltonian systems.

In numerical experiments we have shown that, at any given value of the adiabaticity parameter λ , the value of the maximum Lyapunov exponent in the multiplet of equally-spaced equally-sized resonances is minimal in the doublet case and maximal in the infinity case. This is consistent with the developed theory.

An example of application of the developed theory has been given, concerning asteroidal dynamics in high-order mean motion resonances with Jupiter.

Acknowledgements

The author is thankful to the referee for useful remarks. This work was supported in part by the Programmes of Fundamental Research of the Russian Academy of Sciences “Fundamental Problems in Nonlinear Dynamics” and “Fundamental Problems of the Solar System Studies and Exploration”. The computations were partially carried out at the St. Petersburg Branch of the Joint Supercomputer Centre of the Russian Academy of Sciences.

References

- [1] B.V. Chirikov, *Phys. Rep.* 52 (1979) 263.
- [2] A.J. Lichtenberg, M.A. Lieberman, *Regular and Chaotic Dynamics*, Springer–Verlag, New York, 1992.
- [3] J.D. Meiss, *Rev. Mod. Phys.* 64 (1992) 795.
- [4] S.S. Abdullaev, *Construction of Mappings for Hamiltonian Systems and Their Applications*, Springer, Berlin, 2006.
- [5] I.I. Shevchenko, in: A.Milani, G.B.Valsecchi, and D.Vokrouhlický (Eds.), *Near Earth Objects, our Celestial Neighbors: Opportunity and Risk (Proc. IAU Symp. 236)*, Cambridge Univ. Press, Cambridge, 2007, pp. 15–29.
- [6] I.I. Shevchenko, *Celest. Mech. Dyn. Astron.* 73 (1999) 259.
- [7] I.I. Shevchenko, *Zh. Eksp. Teor. Fiz.* 118 (2000) 707, *JETP* 91 (2000) 615.
- [8] I.I. Shevchenko, *Phys. Scr.* 57 (1998) 185.
- [9] B.V. Chirikov, *Nonlinear Resonance*, Izdatel'stvo NGU, Novosibirsk, 1977, in Russian.
- [10] B.V. Chirikov, D.L. Shepelyansky, *Physica D* 13 (1984) 395.
- [11] I.I. Shevchenko, *Phys. Lett. A* 241 (1998) 53.
- [12] I.I. Shevchenko, *Phys. Lett. A* 372 (2008) 808.
- [13] I.I. Shevchenko, *Astrophys. J.* 733 (2011) 39.
- [14] Cl. Froeschlé, *Celest. Mech.* 34 (1984) 95.
- [15] A. Morbidelli, C. Froeschlé, *Celest. Mech.* 63 (1996) 227.
- [16] D. Nesvorný, A. Morbidelli, *Celest. Mech. Dyn. Astron.* 71 243 (1999).
- [17] M.J. Holman, N.W. Murray, *Astron. J.* 112 (1996) 1278.
- [18] N.W. Murray, M.J. Holman, *Astron. J.* 114 (1997) 1246.

- [19] A. Morbidelli, *Modern Celestial Mechanics*, Taylor and Francis, Padstow, 2002.
- [20] I.I. Shevchenko, *Izvestia GAO* 214 (2000) 153, in Russian.
- [21] I.I. Shevchenko, *Kosmich. Issled.* 40 (2002) 317, *Cosmic Res.* 40 (2002) 296.
- [22] I.I. Shevchenko, *Mon. Not. R. Astron. Soc.* 384 (2008) 1211; *Mon. Not. R. Astron. Soc.* 407 (2010) 704.
- [23] I.I. Shevchenko, *Phys. Lett. A* 333 (2004) 408.
- [24] I.I. Shevchenko, *Pis'ma Zh. Eksp. Teor. Fiz.* 79 (2004) 651, *JETP Lett.* 79 (2004) 523.
- [25] I.I. Shevchenko, *Phys. Rev. E* 85 (2012) 066202.
- [26] S.M. Soskin, R. Mannella, O.M. Yevtushenko, I.A. Khovanov, P.V.E. McClintock, *Fluctuation and Noise Letters* 11 (2012) 1240002.
- [27] V.V. Vecheslavov, B.V. Chirikov, *Zh. Eksp. Teor. Fiz.* 114 (1998) 1516, *JETP* 87 (1998) 823.
- [28] V.V. Vecheslavov, *Zh. Eksp. Teor. Fiz.* 116 (1999) 336, *JETP* 89 (1999) 182.
- [29] V.F. Lazutkin, *J. Math. Sci.* 128 (2005) 2687. (Translated from Russian; originally published in: *VINITI No. 6372/84 (1984).*)
- [30] V.G. Gelfreich, *Commun. Math. Phys.* 201 (1999) 155.
- [31] I.I. Shevchenko, V.V. Kouprianov, *Astron. Astrophys.* 394 (2002) 663.
- [32] V.V. Kouprianov, I.I. Shevchenko, *Icarus* 176 (2005) 224.
- [33] E. Hairer, S.P. Nørsett, G. Wanner, *Solving Ordinary Differential Equations I, Nonstiff Problems*, Springer-Verlag, Berlin, 1987.
- [34] H.F. von Bremen, F.E. Udawadia, W. Proskurowski, *Physica D* 101 (1997) 1.
- [35] V.G. Gelfreich, *Nonlinearity* 10 (1997) 175.

- [36] D.V. Treshchev, *An Introduction to the Perturbation Theory of Hamiltonian Systems*, FAZIS, Moscow, 1998, in Russian.
- [37] A. Milani, A.M. Nobili, *Nature* 357 (1992) 569.
- [38] A. Milani, A.M. Nobili, *Celest. Mech. Dyn. Astron.* 56 (1993) 323.
- [39] K. Tsiganis, H. Varvoglis, J.D.Hadjidemetriou, *Icarus* 146 (2000) 240.
- [40] Z. Knežević, A. Milani, *Astron. Astrophys.* 403 (2003) 1165.
- [41] Z. Knežević, A. Milani, in: *IAU Joint Discussion 7, IAU GA, Beijing, 2012*, p. 18.